FINAL REPORT

Title: Does high-severity patch structure scale consistently with fire size across the Northwest US?

JFSP PROJECT ID: 21-1-01-26

March 2023

Michele S. Buonanduci, Student Investigator

School of Environmental and Forest Sciences

University of Washington

Brian J. Harvey, Principal Investigator

School of Environmental and Forest Sciences

University of Washington

FIRESCIENCE.GOV

Research Supporting Sound Decisions

Table of Contents

List of Tables

List of Figures

List of Abbreviations/Acronyms

ESP: environmental site potential

FRG: fire regime group

RdNBR: relativized differenced normalized burn ratio

SDC: stand-replacing decay coefficient

Keywords

fire regimes; burn severity; high-severity patches; scaling relationships; climate change; stationarity

Acknowledgements

We gratefully acknowledge the contributions of our coauthors and collaborators D. Donato, J. Halofsky, and M. Kennedy. We thank K. Kopper, K. James, V. Wright, and S. Leirfallom for supporting this research. This research funded by the Graduate Research Innovation award (#21-1-01-26) from the Joint Fire Science Program and a U.S. Geological Survey Northwest Climate Adaptation Science Center award G17AC000218 to Michele S. Buonanduci. Brian J. Harvey acknowledges support from the Jack Corkery and George Corkery Jr. Endowed Professorship in Forest Sciences.

Abstract

Across western North America, fire regimes (i.e., the frequency, extent, and severity of fire events) are changing in response to warming climate. Regions in which fire regimes are driven by top-down controls (e.g., climate, fire weather) are likely to see the largest future increases in area burned as climate continues to warm. These climate-limited fire regimes are characterized by infrequent, typically high-severity stand-replacing fire with multi-century fire return intervals and fire events as large as one million hectares in size. Managers working in regions with climate-limited fire regimes are preparing for a warmer, drier future that may bring more frequent, extreme fire events. One need highlighted by managers and punctuated by the widespread west coast fire activity in summer 2020 is an understanding of the historical patch structure of wildfires, particularly the total area burned and high-severity patch size distribution of individual fire events and their range of variation. However, due to the historically infrequent nature of fire in climate-limited fire regimes, information about the size and severity of fire events in these regions is inherently limited.

Using a satellite fire severity dataset of 1,615 fire events occurring across the Northwest US between 1985 and 2020, we present an approach for characterizing burn severity patterns expected within contemporary climate-limited fire regimes. We asked: *(Q1). What is the relationship between overall fire size and high-severity patch structure of contemporary fires (1985-2020) in the Northwest US? (Q2). Does this relationship vary by region, time period, or across a gradient of fuel- to climate-limited fire regimes?* To address Q1, we use nonparametric quantile regression to quantify the range of variation in high-severity burn patch metrics expected across the range of observed fire sizes (400 – >400,000 ha). To address Q2, we test whether the relationships between patch metrics and fire size vary by geographic region (Pacific Northwest versus Northern Rockies), year, time period (1985 – 2000 versus 2001 – 2020), or fire regime (infrequent and high-severity versus moderately frequent and mixed-severity or frequent and low-severity).

We observed: 1) high-severity patches increasing consistently in size and spatial homogeneity with greater fire size within fire regimes, 2) different ranges of variation in scaling relationships among fire regimes, and 3) widely varying distributions of high-severity patches within smaller fires but convergence of patch-size distributions toward a power law function with increasing fire size. Collectively, our results suggest spatial patterns of high-severity fire demonstrate clear and consistent scaling behavior. Within fire regimes, scaling relationships did not differ substantially across space or time, suggesting that as fire size distributions potentially shift under climate change, the stationarity we observed in patch-size scaling can be used to infer expected future patterns of burn severity.

Managing for future fire requires not only projecting possible changes in regional metrics such as annual area burned, but also anticipating the potential ecological impacts of those changes. At broad scales, stationarity in scaling relationships offers a means of projecting the potential range of ecological impacts expected with future fire activity. Continued implementation of the methods presented here would permit changes in scaling relationships to be detected (e.g., downward shifts in scaling relationships might suggest an increasing prevalence of local-scale fuel constraints) that might signal important future changes in the nature of fire regimes.

Objectives

Our objective was to develop an understanding of the high-severity patch structure of wildfires expected with future fire activity in climate-limited fire regimes across the Northwest US. We proposed to address this objective by examining the spatial patterns of contemporary fires (1985-2020) that have occurred across the Northwest US, developing an atlas of scaling relationships that relate high-severity patch size and structure to overall fire size. Our specific research questions were: *(Q1). What is the relationship between overall fire size and high-severity patch structure (mean area-weighted patch size and total core area) of contemporary fires (1985-2020) in the Northwest US? (Q2). Does this relationship vary by region, time period, or across a gradient of fuel- to climate-limited fire regimes?* By evaluating scaling relationships across a broad range of forest ecosystems and fuel- to climate-limited fire regimes, we suggest these scaling relationships can provide insights for managers working in forest ecosystems across the Northwest US.

Our objectives were directly relevant to the JFSP GRIN task statement as the research built on previous research within my PhD that aimed to quantify expected burn severity patch structure in Washington and Oregon. The project also addressed the JFSP topic areas *changing fire environment* and *fire effects and post-fire recovery*. We met all study objectives, and our project methods, findings, and management implications are outlined in this report.

Background

Across western North America, fire regimes (i.e., the frequency, extent, and severity of fire events) are changing in response to warming climate (Westerling *et al.* 2006; Littell *et al.* 2009). The occurrence of large fire events, total area burned, and severity of wildfires have been increasing in recent decades and are strongly associated with warm and dry conditions (Miller *et al.* 2009; Harvey *et al.* 2016a; Westerling 2016). Continued changes in temperature and precipitation patterns, and resultant changes in fire regimes, will have widespread and substantial impacts on Northwest US forests (Halofsky *et al.* 2020).

Fire regimes vary widely across the Northwest US, particularly across drought, aridity, and productivity gradients (Littell *et al.* 2018). For example, in the Pacific Northwest, dry coniferous forests and woodlands east of the Cascade Divide are characterized by fire regimes ranging from frequent and low severity to moderately frequent and mixed severity (Agee 1993; Reilly *et al.* 2021). Conversely, moist coniferous forests west of the Cascade Divide are characterized by infrequent, typically high-severity stand-replacing fire with multi-century fire return intervals and fire events as large as one million hectares in size (Agee 1993; Donato *et al.* 2020; Reilly *et al.* 2021). Similarly, in the Northern Rockies, high elevation cold and/or mesic forests are characterized by infrequent, high-severity fire regimes, while lower elevation forests are characterized by more frequent, mixed-severity regimes (Hood *et al.* 2021). The extent to which these fire regimes are shaped by broad-scale drivers (e.g., climate, fire weather) versus fine-scale constraints (e.g., topography, vegetation) (McKenzie & Kennedy 2011) also varies widely, with ecosystems west of the Cascade Divide and at high elevations in subalpine forests of the Northern Rockies being more climate-limited in general (Littell *et al.* 2018).

As climate warms, the largest future increases in area burned may occur where climate has historically been the limiting factor for fire (Littell *et al.* 2018). In climate-limited and relatively infrequent-fire regimes such as the Western Cascades and subalpine forests of the Northern

Rockies, the relatively rare but extreme nature of fire events poses challenges for forest management (Donato *et al.* 2020). While pre-fire climate adaptation options are perhaps fewer in these ecosystems, management strategies can be implemented both before and after the occurrence of fire to reduce negative impacts on ecosystem services and forest function (Halofsky *et al.* 2018). However, preemptively developing post-fire response plans requires an understanding of the high-severity patch structure of individual fire events, as areas burned at high severity (i.e., areas in which most or all vegetation is killed by fire) are where management intervention is often of greatest priority. Managers in climate-limited fire regimes are preparing for a warmer, drier future that may bring more frequent, extreme fire, while grappling with uncertainties associated with systems where information about disturbances is inherently limited.

Characteristic spatial scaling relationships that relate high-severity patch structure to overall fire size (e.g., following McKenzie & Kennedy 2011; Cansler & McKenzie 2014), when combined with projected increases in area burned, can help managers anticipate future fire impacts. Understanding how high-severity patch structure scales with the size of individual fire events will inform both pre- and post-fire decisions and guide climate-adaptive management across land ownerships (Cansler & McKenzie 2014; Halofsky *et al.* 2018). Using a satellite fire severity dataset of 1,615 fire events occurring across the Northwest US between 1985 and 2020, we present an approach for characterizing burn severity patterns expected within contemporary fire regimes. We ask: *(1). What is the relationship between overall fire size and high-severity patch structure (mean area-weighted patch size and total core area) of contemporary fires (1985-2020) in the Northwest US? (2). Does this relationship vary by region, time period, or across a gradient of fuel- to climate-limited fire regimes?* To anticipate the ecological impacts of future increases in area burned across the Northwest US, understanding not only the relative size of fire events, but also the range of potential high-severity patch structure within those respective fire sizes, will be critical.

Materials and Methods

Study Region

Our study region is the forested ecoregions of the Northwest US (Wyoming, Montana, Idaho, Washington, Oregon, and northern California), delineated using EPA Level III Ecoregions (Commission for Environmental Cooperation 1997) (Fig. 1). Climate, topography, and forest types vary widely across the study region, as do fire activity and fire-adapted traits of dominant tree species (Stevens *et al.* 2020; Hood *et al.* 2021; Reilly *et al.* 2021). Historical fire regimes range from frequent, low-severity fire in warmer and drier parts of the region to infrequent, high-severity fire in cooler and wetter parts of the region (Hood *et al.* 2021; Reilly *et al.* 2021). We used LANDFIRE land cover data to classify forested areas and fire regime groups (FRGs) throughout the study region (Rollins 2009). We identified potentially forested areas using LANDFIRE Environmental Site Potential (ESP) and classified the study region into three historical fire regimes: frequent and low severity (FRG I), moderately frequent and mixed severity (FRG III), and infrequent and high severity (FRG IV and FRG V).

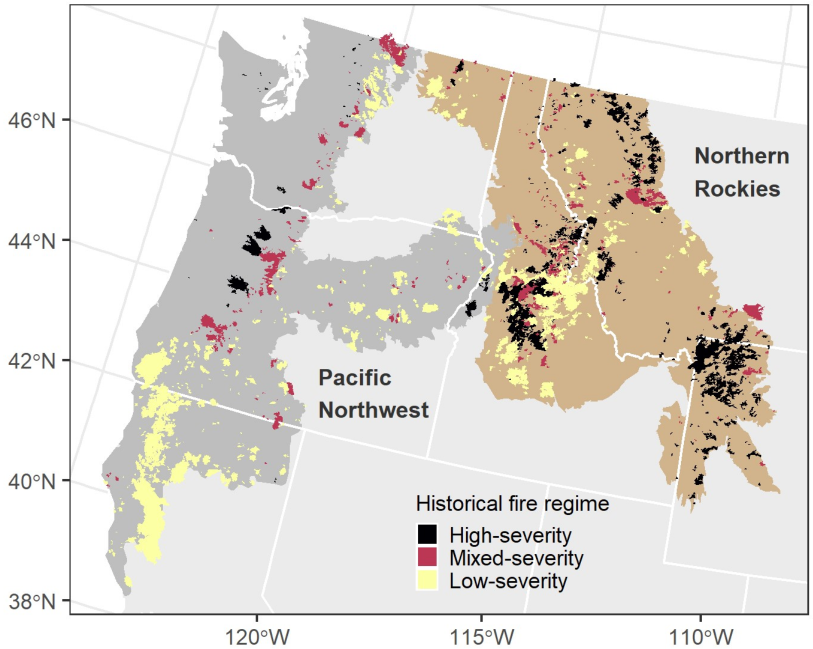

Figure 1. *Study region with all wildfire events categorized by primary historical fire regime (frequent and low-severity, moderately frequent and mixed-severity, infrequent and high-severity).*

Fire Severity Data

We obtained perimeters for all fire events ≥ 400 ha in size occurring within the study region between 1985 and 2020 from the Monitoring Trends in Burn Severity database (https://mtbs.gov/). We included only those fire events occurring in primarily forested areas (≥ 50% forested based on LANDFIRE ESP) that were designated wildfires (i.e., we excluded prescribed fires). Each fire event was assigned its dominant historical fire regime (low-, mixed-, or high-severity) based on the most prevalent fire regime group within that fire's perimeter (Fig. 1). In total, our dataset consisted of 1,615 individual fire events, with 751, 373, and 491 fire events assigned to the low-, mixed-, and high-severity fire regime groups, respectively.

Burn severity maps were generated for each fire event using Landsat satellite data and following previously established methods (Parks *et al.* 2018a). We quantified burn severity at a 30 m pixel scale using the relativized differenced normalized burn ratio (RdNBR), a satellite-based fire severity metric that estimates the amount of fire-induced vegetation change by comparing pre- and post-fire vegetation greenness indices (Miller & Thode 2007). We included an offset term in our calculation of RdNBR to account for phenological differences between pre- and post-fire imagery (Parks *et al.* 2018a). Using statistical models calibrated to Northwest US field plots (Saberi 2019), we identified a threshold of RdNBR (RdNBR ≥ 542) corresponding to ≥75% tree basal area mortality. We then used this threshold to categorize each burn severity map into high (RdNBR ≥ 542) and low-to-moderate (RdNBR < 542) burn severity classes.

Landscape Metrics

Our analysis focused on areas within each fire event that burned at high severity, quantifying landscape metrics describing both the size and spatial configuration of high-severity patches.

High-severity patches were delineated using an eight-neighbor rule after a majority smoothing filter was applied to each categorized burn severity map to reduce the impact of single-pixel patches (Fig. 2A). Within each high-severity patch, distance to seed source was quantified for each pixel that was potentially forested prior to burning. Distance to seed source was quantified by calculating the distance to the nearest potentially forested pixel that did not burn at high severity (Fig. 2B).

We quantified the size of high-severity patches using two complementary approaches (Fig. 2A). First, we calculated the area-weighted mean size of all high-severity patches within each fire event. By weighting larger patches more heavily, an area-weighted mean is larger than an arithmetic mean and represents the expected patch size that would be encountered in an average location within a landscape (Harvey *et al.* 2016a). Second, we characterized the shape of each patch size distribution using an approach that has, to the best of our knowledge, not previously been used to describe high-severity patch size distributions within fire events. Following the methods developed for fire size distributions by Hantson *et al.* (2016), we fit truncated lognormal distributions to the patch sizes within each fire event. The probability density function, *p(x)*, for each patch size distribution takes the following form:

$$\ln p(x) = \ln C - \beta \ln x - \psi [\ln x]^2$$

where C is a normalization constant, ensuring the area under *p(x)* sums to 1, and takes the following form:

$$C = \left(\int_{x_{min}}^{x_{max}} e^{-\beta \ln x - \psi [\ln x]^2} dx \right)^{-1}$$

The parameters *xmin* and *xmax* define the lower and upper truncation limits, respectively. We set *xmin* equal to 1 ha and *xmax* equal to the size of each individual fire event. Essentially, *p(x)* is a modified truncated power law function with an added term, ψ, that adds curvature to the distribution in log-log space (Pueyo 2006). Within the truncation limits, the parameters ψ and β determine the shape of each distribution (Fig. 2A). When ψ is equal to 0, the distribution reduces to a power law function, and the shape of the distribution is a straight line in log-log space, with β determining the slope, or relative prevalence of small versus large patch sizes. When ψ is negative, the distribution curves upward in log-log space (i.e., there is a greater likelihood of large patches, relative to a power law function with the same value of β). When ψ is positive, the distribution curves downward in log-log space (i.e., there is a lower likelihood of large patches, relative to a power law function with the same value of β). In practice, the parameters ψ and β are highly correlated, with β decreasing as ψ increases (Fig. 2A) (Hantson *et al.* 2016).

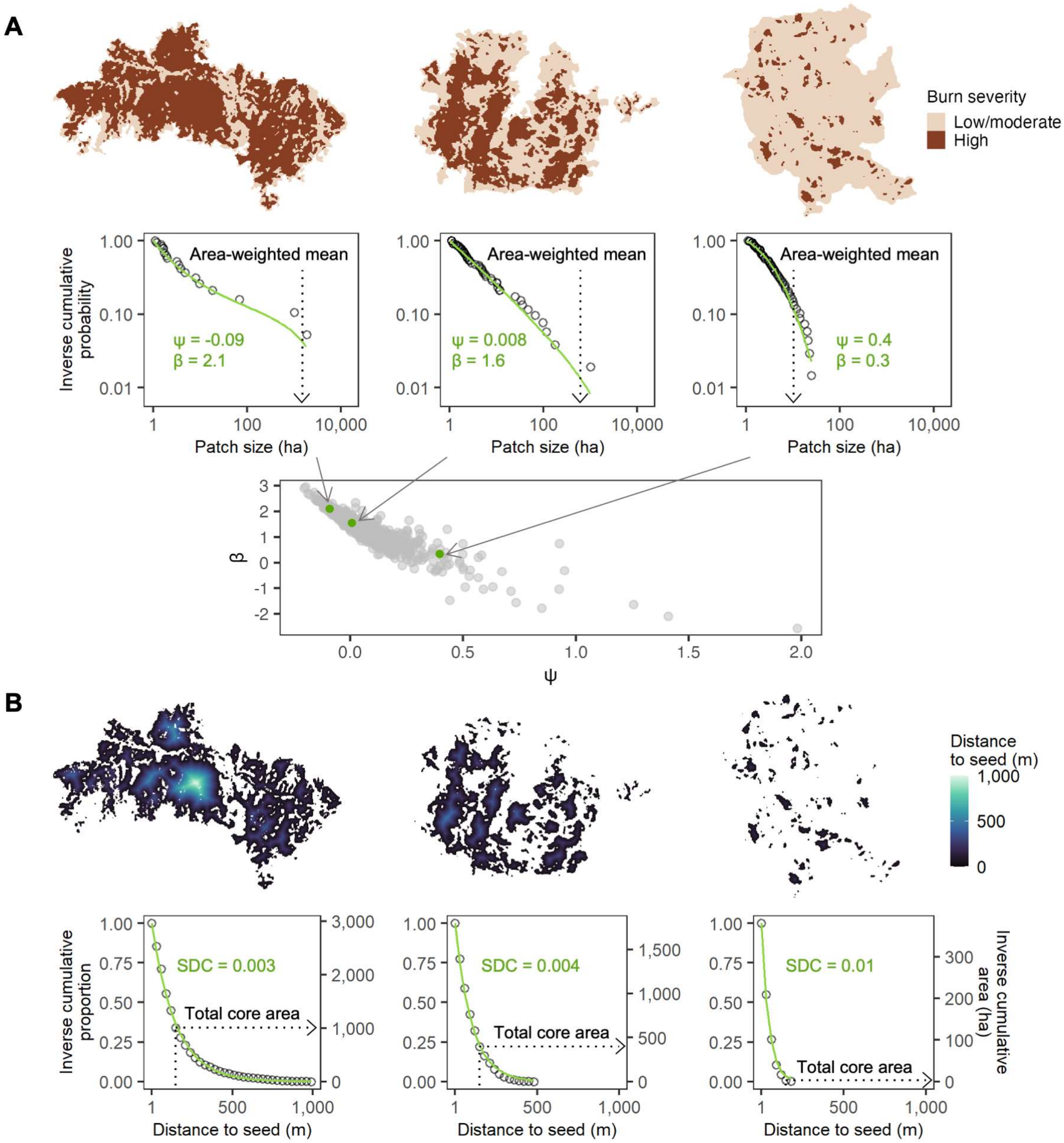

Figure 2. *Schematic illustrating high-severity patch size (A) and high-severity patch structure (B), along with the spatial metrics for each. Open circles represent observed data within each fire event, black dotted lines with arrows point to standard (aggregate or central tendency) metrics, and solid green lines represent metrics describing within-fire distributions. (A) Patch size metrics include area-weighted mean patch size and two parameters (ψ and β) describing the shape of the patch size distribution. Scatter plot of ψ and β shows parameter values for all fires in the dataset. (B) Patch structure metrics account for patch shape and forest cover and include total high-severity core area (previously forested pixels > 150 m from potential unburned seed source following fire) and one parameter (SDC) describing the shape of the distance-to-seed distribution for forested areas burned at high severity. From left to right, example fires include the Fishhawk (Wyoming), Boze (Oregon), and Big Bend (Oregon) fires, which were all 4,000 – 4,500 ha in size.*

As with the size of high-severity patches, we quantified the spatial structure of high-severity patches using two complementary approaches (Fig. 2B). First, we calculated total core area within the interior of high-severity patches, where core area is defined as previously forested pixels $\geq$ 150 m from potential seed source following fire. This threshold of 150 m exceeds the likely seed dispersal distance for many conifers in the Northwest US (Donato *et al.* 2009; Harvey *et al.* 2016b). Second, using the approach proposed by (Collins *et al.* 2017), we characterized the rate at which the forested area within the interior of high-severity patches shrinks with increasing distance to potential seed source. In this approach, the proportion of total high-severity or "stand-replacing" forested area, *P*, exceeding a given distance to potential seed, *dist*, is modeled using a modified logistic function as follows:

$$P \sim \frac{1}{10^{SDC\ x\ dist}}$$

Here, the stand-replacing decay coefficient (SDC) is a parameter determining the rate at which the proportional stand-replacing area decreases with increasing distance to potential seed. Larger values of SDC indicate a rapidly decaying interior area (i.e., most forested areas burned at high severity are relatively close to potential seed sources), whereas smaller values of SDC indicate a more slowly decaying interior area (i.e., more forested areas burned at high severity are far from potential seed sources) (Collins *et al.* 2017).

Area-weighted mean patch size and total core area were calculated using the *sf* and *raster* packages in R (Pebesma 2018; Hijmans *et al.* 2022). Patch size distribution shape parameters (ψ and β) were fit to the patch size distributions for each fire event using the maximum likelihood algorithm proposed by Pueyo (2014). We only fit patch size distribution parameters for fire events with at least 10 patches exceeding 1 ha in size. Distance-to-seed distribution parameters (SDC) were fit to the inverse cumulative distance-to-seed distributions for each fire event using nonlinear least squares, following Collins *et al.* (2017). Inverse cumulative distance-to-seed distributions were summarized using 30 m bins of pixel-level distance to potential seed source prior to parameter fitting.

Analysis

We used nonparametric quantile regression to quantify the range of variation in high-severity patch size and structure metrics expected from fires of different sizes (Q1). Compared to standard regression approaches, which estimate the conditional mean of a response variable, quantile regression estimates the conditional quantiles of a response variable, thereby providing a fuller picture of the relationships between variables (Koenker & Bassett 1978; Cade & Noon 2003). This approach is particularly useful in ecological applications where complex interactions between multiple variables, many of which cannot be accounted for, lead to unequal variances in response distributions (Cade & Noon 2003). Rather than assuming linearity in scaling relationships, we used a nonparametric approach to fit smooth curves (via additive basis splines) to the conditional quantiles of each scaling relationship (Muggeo *et al.* 2021).

We fit smooth curves to five conditional quantiles (0.05, 0.25, 0.5, 0.75, and 0.95) of each patch size and structure metric across the range of observed fire sizes within each fire regime. Quantile curves were constrained to be monotonically increasing for area-weighted mean patch size and total core area, both of which are expected to continually increase with fire size (Harvey *et al.* 2016a; Reilly *et al.* 2017; Stevens *et al.* 2017), and monotonically decreasing for the distance-to-seed parameter (SDC), which is expected to continually decrease with fire size (Collins *et al.*

2017). No monotonicity constraints were imposed for the patch size distribution parameters (ψ and β). Area-weighted mean patch size, total core area, and SDC were $\log_{10}$-transformed prior to model fitting; in cases where total core area was zero, we added 0.01 ha to enable $\log_{10}$-transformation. To evaluate potential differences between fire regimes, we also fit combined models for each metric with smooth terms for fire size that were allowed to vary by fire regime. We then evaluated whether there were significant differences between fire regime-specific scaling relationships by calculating pointwise differences, along with approximate 95% confidence intervals, between pairs of regime-specific quantile curves across the range of observed fire sizes following Rose *et al.* (2012). All quantile curves were fit using the *quantregGrowth* package in R (Muggeo 2021).

We used multiple lines of evidence to evaluate the spatial and temporal stationarity of scaling relationships (Q2). To evaluate spatial stationarity, we considered two broad geographic regions within our study area: the Pacific Northwest and the Northern Rockies (Fig. 1). Unfortunately, within the high-severity fire regime, there were too few fire events in the Pacific Northwest ($n = 42$) for a robust comparison with the Northern Rockies ($n = 449$) (Tables 1, 2). Within the low- and mixed-severity fire regimes, however, we fit quantile regression models with smooth terms for fire size that were allowed to vary by geographic region. We then evaluated whether there were significant differences between region-specific scaling relationships by calculating pointwise differences between region-specific quantile curves, along with approximate 95% confidence intervals, following the approach used for fire regimes.

To evaluate temporal stationarity, we considered annual trends as well as two distinct time periods: an early period (1985 – 2000) and a late period (2001 – 2020), the latter of which is associated with increasing aridity and accelerating annual area burned in the western US (Juang *et al.* 2022). Within each fire regime, we fit three sets of quantile regression models. First, to assess interannual variation, we fit models with smooth terms for fire size and additional smooth terms for year. Second, to test for overall increasing or decreasing trends, we fit models with smooth terms for fire size and additional linear terms for year. Annual trends were considered statistically significant if $p < 0.05$ for the linear year term. Third, to evaluate whether there were significant differences between time period-specific scaling relationships, we fit quantile regression models with smooth terms for fire size that were allowed to vary by time period, following the approach used for fire regimes and geographic regions.

As an additional line of evidence, we used a 10-fold cross-validation procedure to evaluate whether adding a smooth term for year or allowing scaling relationships to vary either by time period or geographic region improved model predictive power over a null model (i.e., a model including fire size as the only predictor). Prediction error was calculated for quantiles 0.05, 0.5, and 0.95 using the quantile loss function (Koenker & Bassett 1978), which asymmetrically weights the absolute residuals and is analogous to the root mean square error used in standard regression models. Prediction error was averaged across quantiles and cross-validation folds for each model, with a reduction in overall average prediction error considered an improvement in model predictive power.

Table 1. *Summary statistics for high-severity patch size metrics.*

Fire regime group	Region	Time period	n	Area-weighted mean (ha) n	Min	Max	Median	Mean	β parameter n	Min	Max	Median	Mean	ψ parameter n	Min	Max	Median	Mean
High	Combined	Combined	491	490	3.5	16,738	286	995	356	-1.78	2.74	1.36	1.35	356	-0.19	0.85	0.03	0.04
	N. Rockies	Combined	449	449	6.1	16,738	313	972	328	-1.78	2.74	1.38	1.36	328	-0.19	0.85	0.03	0.04
	P. Northwest	Combined	42	41	3.5	14,454	104	1,255	28	0.14	2.13	1.26	1.23	28	-0.12	0.25	0.06	0.07
	Combined	Early	144	143	3.5	16,738	228	897	100	-1.78	2.44	1.38	1.32	100	-0.15	0.85	0.03	0.05
	Combined	Late	347	347	7.9	15,227	300	1,036	256	-0.27	2.74	1.35	1.36	256	-0.19	0.42	0.03	0.04
Mixed	Combined	Combined	373	372	0.2	20,418	176	855	266	-2.57	2.90	1.40	1.32	266	-0.20	1.98	0.03	0.06
	N. Rockies	Combined	211	210	0.3	18,509	170	639	147	-0.37	2.47	1.40	1.38	147	-0.14	0.41	0.03	0.05
	P. Northwest	Combined	162	162	0.2	20,418	194	1,136	119	-2.57	2.90	1.39	1.25	119	-0.20	1.98	0.04	0.09
	Combined	Early	99	98	0.8	18,509	239	748	65	-1.57	2.47	1.39	1.27	65	-0.14	0.74	0.03	0.06
	Combined	Late	274	274	0.2	20,418	165	893	201	-2.57	2.90	1.40	1.33	201	-0.20	1.98	0.04	0.07
Low	Combined	Combined	751	747	0.2	28,602	153	772	531	-2.10	2.95	1.35	1.27	531	-0.20	1.41	0.05	0.08
	N. Rockies	Combined	261	259	0.4	17,374	114	690	187	-2.10	2.64	1.38	1.29	187	-0.15	1.41	0.04	0.08
	P. Northwest	Combined	490	488	0.2	28,602	182	816	344	-1.64	2.95	1.31	1.25	344	-0.20	1.26	0.05	0.09
	Combined	Early	252	250	0.4	14,345	158	695	174	-2.10	2.95	1.34	1.22	174	-0.20	1.41	0.05	0.09
	Combined	Late	499	497	0.2	28,602	152	811	357	-1.13	2.64	1.35	1.29	357	-0.15	0.95	0.05	0.08

Table 2. *Summary statistics for high-severity patch structure metrics.*

Fire regime group	Region	Time period	n	Total core area (ha)					SDC parameter				
				n	Min	Max	Median	Mean	n	Min	Max	Median	Mean
High	Combined	Combined	491	491	0	41,569	127	894	490	0.0013	0.0153	0.0044	0.0047
	N. Rockies	Combined	449	449	0	41,569	138	863	449	0.0013	0.0143	0.0043	0.0046
	P. Northwest	Combined	42	42	0	16,212	63	1,228	41	0.0018	0.0153	0.0053	0.0059
	Combined	Early	144	144	0	41,569	86	980	143	0.0017	0.0153	0.0045	0.0049
	Combined	Late	347	347	0	18,137	138	858	347	0.0013	0.0124	0.0043	0.0047
Mixed	Combined	Combined	373	373	0	21,052	88	665	370	0.0013	0.0427	0.0049	0.0060
	N. Rockies	Combined	211	211	0	21,052	85	510	209	0.0015	0.0427	0.0049	0.0062
	P. Northwest	Combined	162	162	0	17,143	94	869	161	0.0013	0.0238	0.0048	0.0056
	Combined	Early	99	99	0	21,052	99	523	98	0.0015	0.0321	0.0044	0.0058
	Combined	Late	274	274	0	17,143	84	717	272	0.0013	0.0427	0.0051	0.0060
Low	Combined	Combined	751	751	0	66,319	85	825	742	0.0008	0.0312	0.0051	0.0062
	N. Rockies	Combined	261	261	0	16,427	57	691	256	0.0009	0.0279	0.0053	0.0064
	P. Northwest	Combined	490	490	0	66,319	103	897	486	0.0008	0.0312	0.0049	0.0061
	Combined	Early	252	252	0	16,427	81	541	248	0.0008	0.0305	0.0047	0.0057
	Combined	Late	499	499	0	66,319	86	969	494	0.0008	0.0312	0.0052	0.0064

Results and Discussion

Scaling Relationships

Within Fire Regimes

Within fire regimes, high-severity patch size and structure demonstrated clear scaling relationships (Fig. 3A–J). With greater fire size, high-severity patches tended to be larger and more spatially homogenous (greater area-weighted mean patch size and total core area; Fig. 3A,B,G,H), containing areas that were increasingly far from potential seed sources (lower SDC; Fig. 3I,J). In forested ecosystems that rely on seed dispersal for post-fire recovery, larger and more homogenous high-severity patches can alter forest resilience, as they are more likely to regenerate slowly and to persist in a non-forest state following fire (Coop *et al.* 2020). Overall, we found that scaling relationships for high-severity patch size and structure were qualitatively similar across fire regimes, demonstrating that across contemporary forest systems, larger fires consistently result in larger and more homogenous patches of high-severity fire.

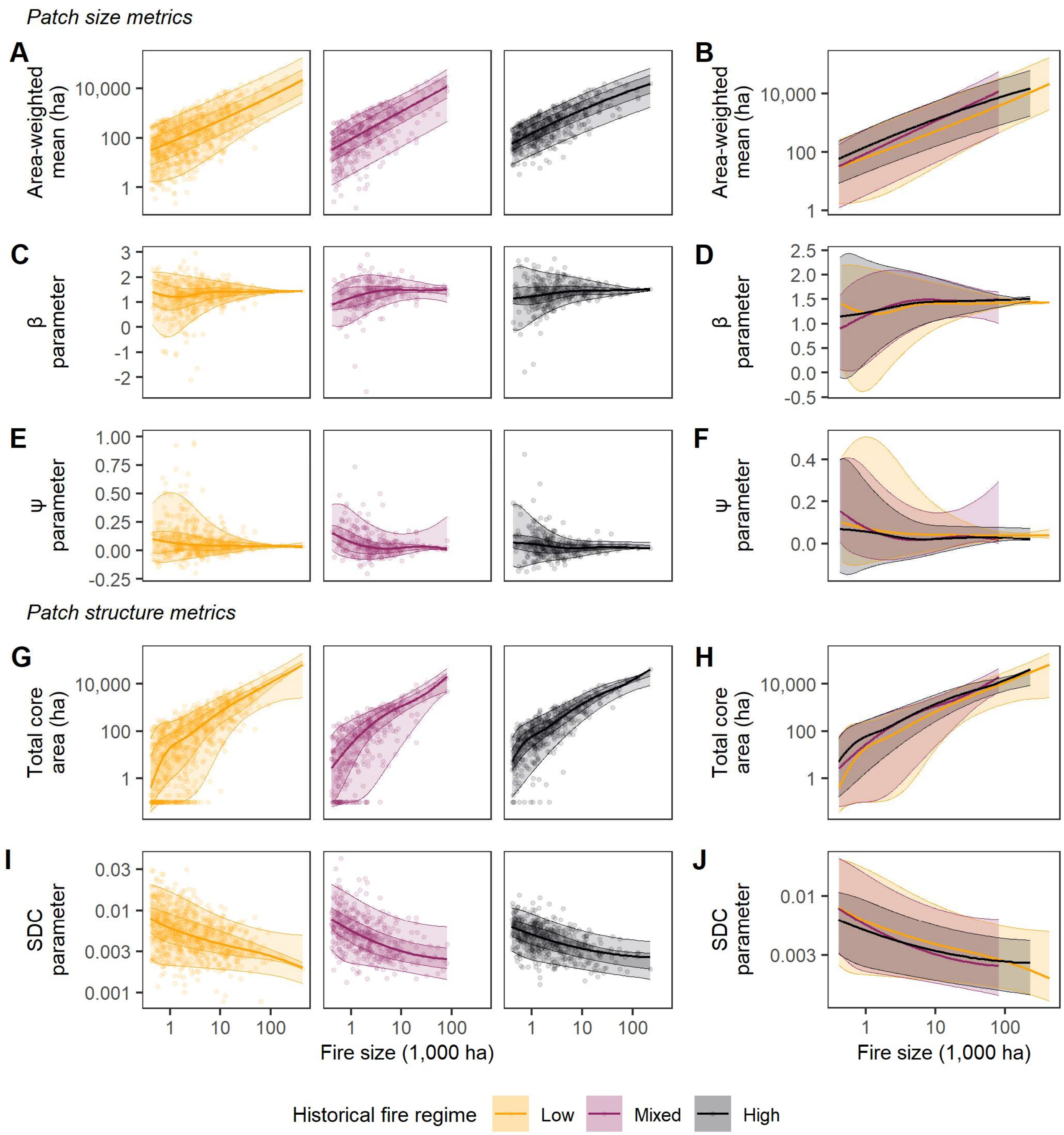

Figure 3. *Quantile regression estimates for all (A – F) high-severity patch size and (G – J) high-severity patch structure metrics, plotted separately for each fire regime with observed data (left column) and overlaid for comparison across regimes (right column). Dots represent observed data, thick solid line is quantile 0.5, dark shaded region is interval between quantiles 0.25 and 0.75 (shown only in plots with observed data), and light shaded region is interval between quantiles 0.05 and 0.95. Three data points (for which $\psi > 1$) were excluded from (E) to improve visualization of quantile estimates.*

Within-fire patch size distributions were highly variable at small fire sizes but converged toward a power law function with increasing fire size (ψ converged toward 0 and β converged toward 1.5; Figs. 2A, 3C–F), carrying implications for the drivers of large fire events. At broad scales (e.g., in the context of regional or global fire size distributions), power law behavior has been posited to emerge within facets of fire activity when there is a balance between broad-scale drivers and local-scale constraints (Moritz *et al.* 2011; McKenzie & Kennedy 2012; Povak *et al.* 2018). Here, the emergence of power law behavior for within-fire patch size distributions suggests that a similar balance may occur within fire events. For small- to moderately-sized fire events (e.g., 400 – 10,000 ha), patch size distributions varied widely, with some fires characterized primarily by large patches and others primarily by small patches (Figs. 2A, 3C–F). This suggests that in smaller fires, either broad- or local-scale factors alone may primarily drive spatial patterns of burn severity. Conversely, the convergence of patch size distributions toward a power law function with increasing fire size suggests that both broad- and local-scale factors influence spatial patterns of burn severity within large fire events (e.g., >10,000 ha). Large fire events often coincide with (Clarke *et al.* 2020; Abatzoglou *et al.* 2021) or can create their own (Fromm *et al.* 2010) extreme weather conditions, driving extreme fire behavior. The largest burn days and largest high-severity patches therefore occur when broad-scale drivers dominate (Peters *et al.* 2004). However, large fires can also burn over the course of many days to weeks (Scaduto *et al.* 2020), spanning a range of weather conditions and, by nature of covering large areas, encounter a range of topographic and vegetation structures. This wide range of conditions, alternating between places and times when broad- versus local-scale factors dominate, allows for the formation of a wide range of patch sizes, including many that are small but also some that are very large.

Although patch size distributions within very large fires consistently converged toward a probability distribution taking the form of a power law, exact patch sizes still varied among fires. Differences in the sizes of the largest patches within fires in particular, along with differences in their spatial structure, can lead to a wide range of ecological impacts. This variation is evident in scaling relationships for the distance-to-seed parameter (SDC), which did not converge toward a particular value with increasing fire size (Fig. 3I,J). The lack of convergence in SDC suggests that even in the largest fires, ecological impacts can vary widely, both due to the size as well as the configuration (i.e., shape and surrounding forest cover) of the largest patches. Despite occurring at the lowest frequency, the largest high-severity patches have the greatest ecological impact, both in terms of total high-severity burned area as well as distances to seed sources within patch interiors (Cansler & McKenzie 2014; Harvey *et al.* 2016a; Collins *et al.* 2017).

Among Fire Regimes

Quantifying multiple conditional quantiles of patch size and structure allowed for a multi-faceted evaluation of scaling relationships both within and among fire regimes. The fire regimes in our study span a gradient of climate- to fuel-limited systems, with fire activity in the infrequent, high-severity fire regime being primarily climate-limited and fire activity in the frequent, low-severity fire regime being primarily fuel-limited (Agee 1993; Baker 2009; Reilly *et al.* 2017; Hood *et al.* 2021). In the absence of other limiting factors, fire size itself imposes some natural upper limit to the size and homogeneity of high-severity burn patches. As limitations on fire severity increase in number and/or relative influence (e.g., in landscapes with complex topography, discontinuous fuel structure, and/or moderate fire weather conditions), patch size and structure are expected to become smaller in size or more complex in shape (Cansler & McKenzie 2014; Harvey *et al.* 2016a), therefore falling below the fire-size-imposed upper limits.

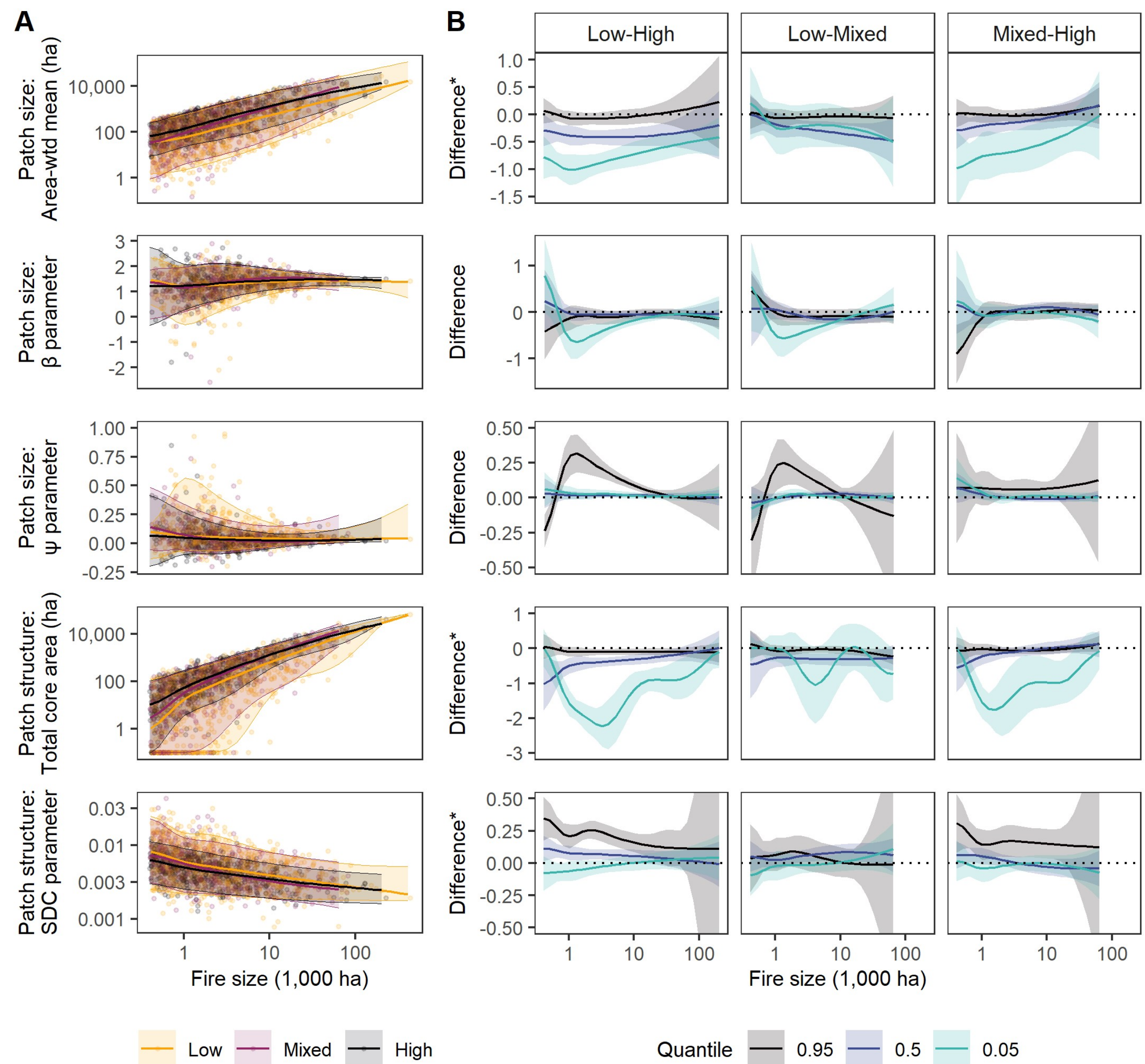

Figure 4. *(A) Quantile regression estimates where each quantile curve is allowed to vary by fire regime. Solid line is quantile 0.5 and shaded region is interval between quantiles 0.05 and 0.95. (B) Estimated differences between quantile curves (solid lines) with 95% confidence intervals (shaded regions). Asterisks (*) indicate differences are on a log10-transformed scale.*

Among fire regimes, the ranges of variation in scaling relationships reveal key similarities and differences in burn severity patterns across systems. Across the range of fire sizes, the upper bounds for potential patch size and homogeneity (i.e., upper quantile estimates for area-weighted mean patch size and total core area, and lower quantile estimates for SDC) did not differ across fire regimes (Fig. 3B,H,J, Fig. 4). This shared upper bound for scaling relationships suggests that when the influence of local-scale constraints is relatively weak (e.g., under extreme fire weather conditions), fire size imposes a comparable upper limit to patch size and structure across systems. Conversely, scaling relationships diverged across fire regimes at the lower bounds for potential patch size and homogeneity (i.e., lower quantile estimates for area-weighted mean patch size and total core area, and upper quantile estimates for SDC; Fig. 3B,H,J, Fig. 4), with patches in the low- and mixed-severity regimes falling below the fire-size-imposed upper limits more frequently than in the high-severity regime. The differing lower bounds for scaling relationships across fire regimes reflect the greater influence of local-scale constraints on fire severity in the low- and mixed-severity systems.

Contemporary ranges of variation in scaling relationships likely differ from historical ranges, particularly in the low- and mixed-severity regimes, due in large part to contemporary land management practices. Forests across the Northwest US have been subject to more than a century of fire suppression (Hagmann *et al.* 2021), which we expect influences scaling relationships in multiple ways. First, since fire suppression efforts are less successful under extreme weather conditions (Arienti *et al.* 2006), the largest fires in our dataset are more likely to have burned under extreme conditions. In the absence of suppression efforts, we might expect to see a wider range of burn severity patterns for larger fires allowed to burn under mild or moderate weather conditions. Second, in low- and mixed-severity regimes, fire exclusion has led to an uncharacteristic buildup of fuels and a misalignment of forest structure and fire activity with historical conditions (Hagmann *et al.* 2021). Prior to European colonization, the low-severity regime was characterized predominantly by frequent but low-severity surface fires that would have resulted from a combination of lightning- and human-ignited fires (Hood *et al.* 2021; Reilly *et al.* 2021). Although we found that burn severity patterns tended to be more heterogeneous in the low-severity regime, we also found that high-severity patches could be as large and homogenous as those observed in the high-severity regime, potentially reflecting this departure from historical conditions. This departure is a major concern for forest resilience in historically low-severity regimes, which are generally not as well adapted to recover from large patches of high-severity fire as are forests within high-severity regimes (Pausas *et al.* 2017; Stevens *et al.* 2020).

Spatial and Temporal Stationarity in Scaling Relationships

Across Northwest US fire regimes and within the contemporary satellite record (1985 – 2020), scaling relationships relating high-severity patch size and structure to fire size appear stationary in both space and time. Region-specific scaling relationships (Pacific Northwest versus Northern Rockies; Fig. 1) largely did not differ within the low- and mixed-severity regimes (for which data were sufficient for a robust regional comparison) (Fig. 5), suggesting that fire regimes are characterized by consistent scaling relationships across space. We observed modest interannual variation in scaling relationships in the low- and mixed-severity regimes (Fig. 6); however, in most cases, linear terms for year were not statistically significant (Fig. 6), and time period-specific scaling relationships [early (1985 – 2000) versus late (2001 – 2020)] largely did not differ (Fig. 7), suggesting the relationships between spatial patterns of burn severity and fire size are not yet changing over time and with warming conditions. Cross-validation indicated that null models (i.e., models including fire size as the only predictor) offered the highest predictive power in most cases (Tables 3, 4); in cases where region, year, or time period did improve model performance, the improvement was slight (prediction error reduced by <1% compared to null models).

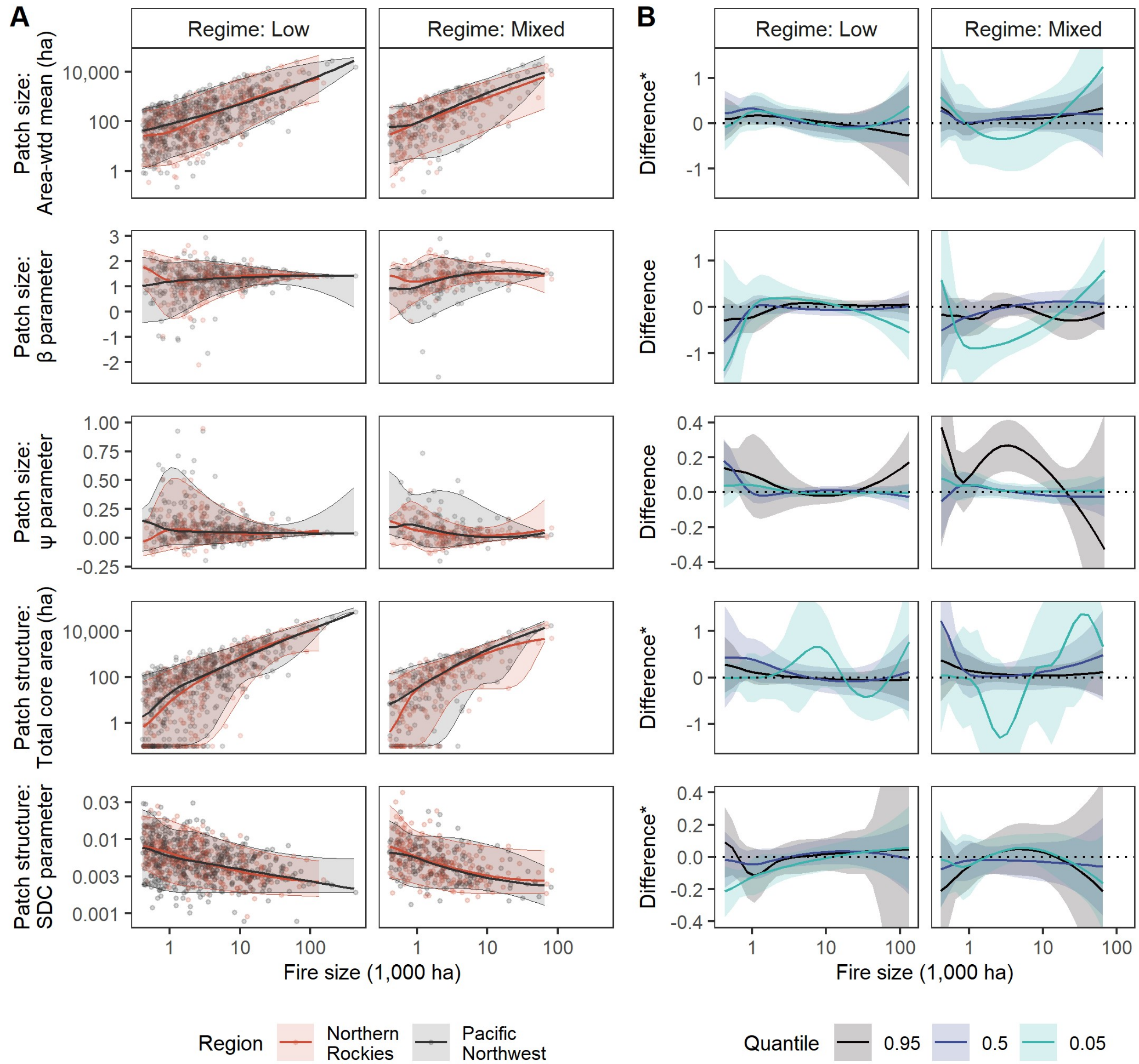

Figure 5. *(A) Quantile regression estimates where each quantile curve is allowed to vary by geographic region. Solid line is quantile 0.5 and shaded region is interval between quantiles 0.05 and 0.95. (B) Estimated differences between quantile curves (Pacific Northwest minus Northern Rockies; solid lines) with 95% confidence intervals (shaded regions). Asterisks (*) indicate differences are on a log10-transformed scale. Within the high severity fire regime, there were too few fire events in the Pacific Northwest (n = 42) for a robust comparison with the Northern Rockies (n = 449).*

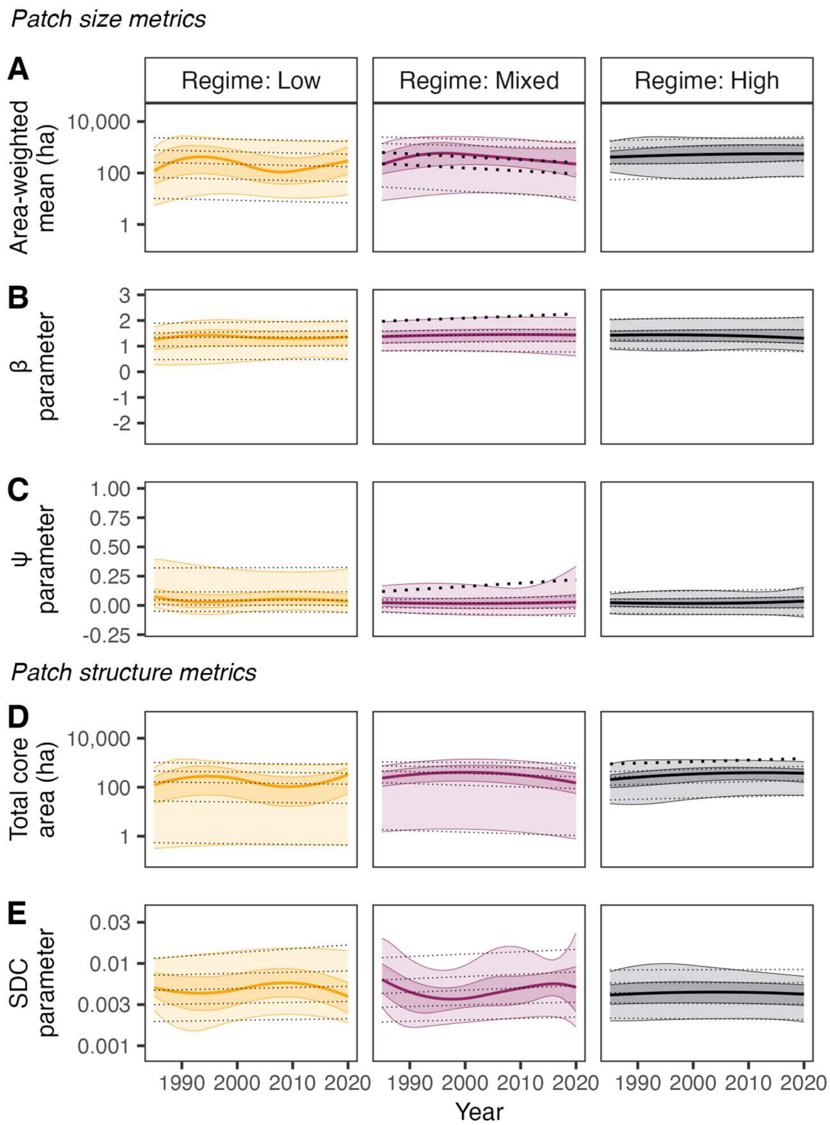

Figure 6. *Estimated marginal effect of year for all metrics. Fire size is held constant at 3,000 ha. Solid lines and shaded intervals are quantile estimates from models with smooth term for year; solid line is quantile 0.5, dark shaded region is interval between quantiles 0.25 and 0.75, and light shaded region is interval between quantiles 0.05 and 0.95. Dotted lines are quantile estimates from models with linear term for year; heavy dotted lines indicate linear terms for which p < 0.05 and light dotted lines indicate linear terms for which p > 0.05. Linear terms were generally not statistically significant, suggesting temporal stationarity in the relationship between fire size and spatial patterns of burn severity.*

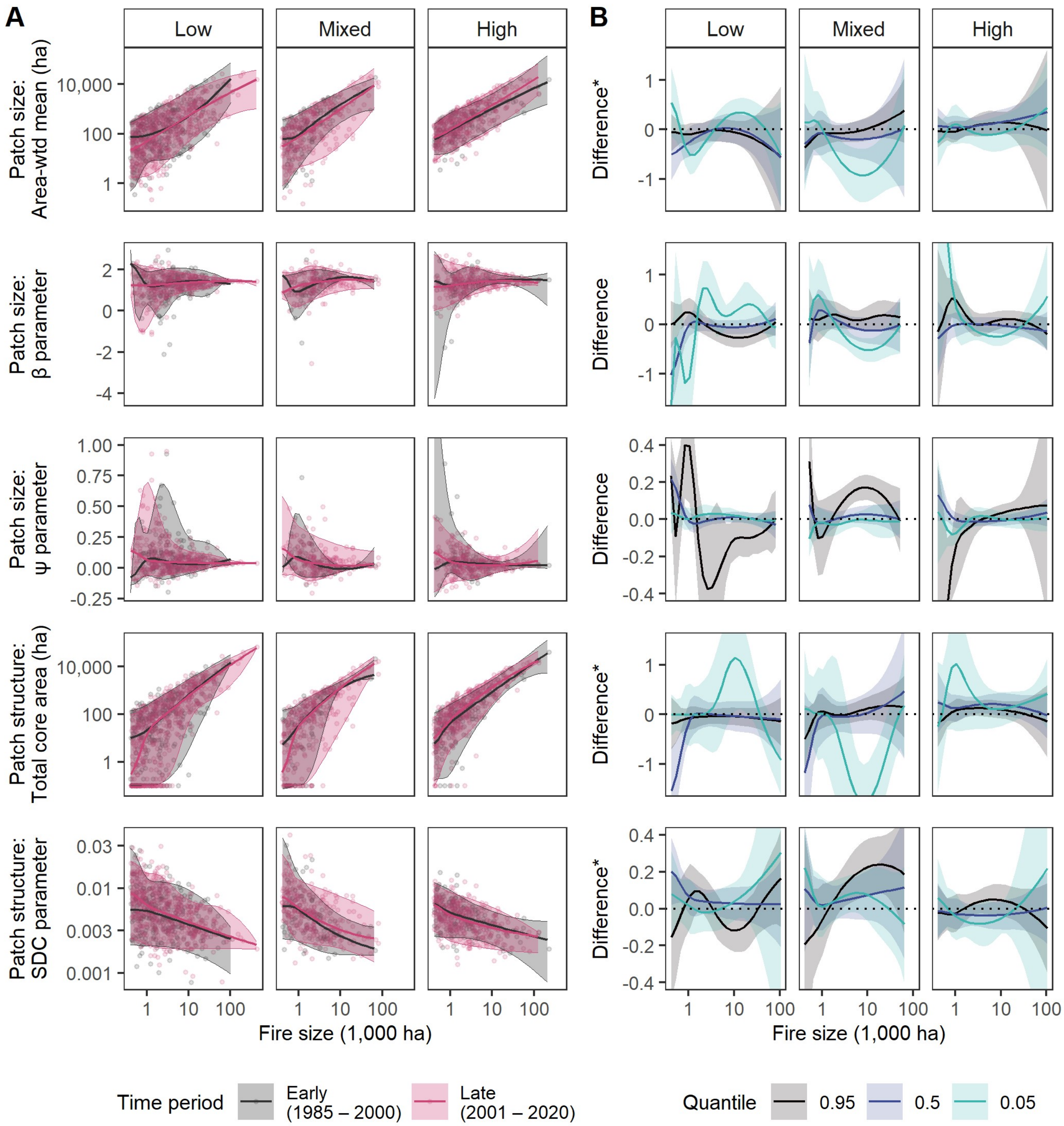

Figure 7. *(A) Quantile regression estimates where each quantile curve is allowed to vary by time period. Early period is defined as 1989 – 2000 and Late period is defined as 2001 – 2020. Solid line is quantile 0.5 and shaded region is interval between quantiles 0.05 and 0.95. (B) Estimated differences between quantile curves (Late minus Early; solid lines) with 95% confidence intervals (shaded regions). Asterisks (*) indicate differences are on a log10-transformed scale.*

Table 3. *Cross-validation results for evaluation of region. Two region-specific model formulations were evaluated: one in which a combined model was fit to the data, within which quantile curves were allowed to vary by region ("1 model"), and another in which separate models were fit to each region ("2 models"). The highest ranked model for each combination of metric and fire regime is emphasized with bold font. Within the high-severity fire regime, there were too few fire events in the Pacific Northwest (n = 42) for a robust comparison with the Northern Rockies (n = 449).*

Metric	Fire regime	Model rank	Model	Average quantile loss
Area-weighted mean	Low	**1**	**null**	**0.1432**
		2	region (2 models)	0.1434
		3	region (1 model)	0.1438
	Mixed	**1**	**null**	**0.1374**
		2	region (2 models)	0.1410
		3	region (1 model)	0.1418
β parameter	Low	**1**	**region (2 models)**	**0.0992**
		2	region (1 model)	0.1000
		3	null	0.1000
	Mixed	**1**	**null**	**0.1015**
		2	region (2 models)	0.1036
		3	region (1 model)	0.1050
ψ parameter	Low	**1**	**null**	**0.0246**
		2	region (1 model)	0.0251
		3	region (2 models)	0.0251
	Mixed	**1**	**null**	**0.0237**
		2	region (2 models)	0.0240
		3	region (1 model)	0.0249
Total core area	Low	**1**	**region (2 models)**	**0.1948**
		2	region (1 model)	0.1950
		3	null	0.1952
	Mixed	**1**	**null**	**0.1779**
		2	region (2 models)	0.1786
		3	region (1 model)	0.1794
SDC parameter	Low	**1**	**null**	**0.0483**
		2	region (2 models)	0.0483
		3	region (1 model)	0.0486
	Mixed	**1**	**null**	**0.0455**
		2	region (1 model)	0.0460
		3	region (2 models)	0.0463

Table 4. *Cross-validation results for evaluation of year and time period. Two time period-specific model formulations were evaluated: one in which a combined model was fit to the data, within which quantile curves were allowed to vary by time period ("1 model"), and another in which separate models were fit to each time period ("2 models"). The highest ranked model for each combination of metric and fire regime is emphasized with bold font.*

Metric	Fire regime	Model rank	Model	Average quantile loss
Area-weighted mean	Low	**1**	**time period (2 models)**	**0.1423**
		2	year	0.1424
		3	time period (1 model)	0.1426
		4	null	0.1429
	Mixed	**1**	**null**	**0.1369**
		2	year	0.1385
		3	time period (2 models)	0.1389
		4	time period (1 model)	0.1393
	High	**1**	**null**	**0.0930**
		2	time period (2 models)	0.0931
		3	time period (1 model)	0.0943
		4	year	0.0944
β parameter	Low	**1**	**null**	**0.1006**
		2	time period (2 models)	0.1015
		3	year	0.1028
		4	time period (1 model)	0.1033
	Mixed	**1**	**null**	**0.1045**
		2	time period (1 model)	0.1047
		3	time period (2 models)	0.1053
		4	year	0.1078
	High	**1**	**year**	**0.0887**
		2	null	0.0892
		3	time period (2 models)	0.0950
		4	time period (1 model)	0.0974
ψ parameter	Low	**1**	**time period (2 models)**	**0.0246**
		2	null	0.0247
		3	year	0.0253
		4	time period (1 model)	0.0255
	Mixed	**1**	**null**	**0.0241**
		2	time period (2 models)	0.0246
		3	year	0.0248
		4	time period (1 model)	0.0251
	High	**1**	**null**	**0.0174**
		2	year	0.0176
		3	time period (2 models)	0.0186
		4	time period (1 model)	0.0190

Metric	Fire regime	Model rank	Model	Average quantile loss
Total core area	Low	**1**	**time period (1 model)**	**0.1944**
		2	year	0.1946
		3	time period (2 models)	0.1952
		4	null	0.1953
	Mixed	**1**	**null**	**0.1778**
		2	year	0.1802
		3	time period (1 model)	0.1810
		4	time period (2 models)	0.1811
	High	**1**	**null**	**0.1154**
		2	time period (2 models)	0.1171
		3	time period (1 model)	0.1176
		4	year	0.1190
SDC parameter	Low	**1**	**year**	**0.0479**
		2	time period (1 model)	0.0482
		3	time period (2 models)	0.0483
		4	null	0.0484
	Mixed	**1**	**year**	**0.0457**
		2	null	0.0458
		3	time period (1 model)	0.0460
		4	time period (2 models)	0.0461
	High	**1**	**null**	**0.0326**
		2	year	0.0330
		3	time period (2 models)	0.0331
		4	time period (1 model)	0.0332

Overall, these lines of evidence suggest both spatial and temporal stationarity in scaling relationships across a wide range of fire regimes and forest ecosystems, even over a time period where climate and fire size distributions themselves were temporally variable (Juang *et al.* 2022). Put plainly, even as fire size distributions have shifted toward larger fires, the ranges of burn severity patterns expected for fires of a given size have remained the same. As climate and fire activity continue to shift, and as fuel limitations potentially increase in areas subject to increasing fire activity (Kennedy *et al.* 2021; Turner *et al.* 2022), it is possible that the envelopes of potential burn severity patterns may shift in the future. Continued implementation of the methods presented here would permit such changes to be detected (e.g., downward shifts in scaling relationships might suggest an increasing prevalence of local-scale fuel constraints, thereby signaling potentially important changes in fire regimes). Within the contemporary fire record, however, our findings suggest that systematic shifts in scaling relationships have not yet occurred.

Managing for future fire requires not only projecting possible changes in regional metrics such as annual area burned, but also anticipating the potential ecological impacts of those changes. At broad scales, stationarity in scaling relationships offers a means of projecting the potential range of ecological impacts expected with future fire activity. Predicting burn severity for a given landscape can be difficult, since fire behavior is highly stochastic and weather conditions at the time of burning can strongly influence the burn severity patterns that result (Parks *et al.* 2018b; Prichard *et al.* 2020). However, by combining the range of variation in scaling relationships with projections for area burned and fire size distributions, it is possible to quantify the range of potential ecological impacts of fire activity at a broader scale. Shifts in fire size distributions alone (i.e., increasing frequency of large fire events) will lead to predictable shifts in ecological impacts (i.e., larger high-severity patches with interior burned areas far from potential seed sources). Accounting for expected patterns of high-severity patch size and structure with increasing fire size enables bounds to be placed around potential outcomes, improving the ability to prepare for future fire impacts.

Science Delivery Activities

Our team was fortunate to have the input of managers from several agencies during the project design phase. Joshua Halofsky (Washington DNR Natural Resource Scientist), Daniel Donato (Washington DNR Natural Resource Scientist), Karen Kopper (North Cascades NP Fire Ecologist), and Kevin James (Mt. Baker-Snoqualmie National Forest Ecologist) provided valuable input regarding data needs, study areas, and fire histories. Vita Wright (NRFSN Science Delivery Specialist) and Signe Leirfallom (NRFSN Coordinator) expressed a strong interest in the outcomes of the project for management of climate-limited forests within their region. Through preparation of reports and fact sheets, the data and results from this project will aid managers in preparing for the ecological impacts of future fire activity.

We have presented the findings of this research to multiple audiences, including the 2021 International Fire Ecology and Management Congress and the 2022 University of Washington Quantitative Seminar Series. We also presented this work in February 2023 at the Oregon Post-Fire Research and Monitoring Symposium, a meeting attended by natural resource professionals, science providers, policy makers, and the general public. We authored a report including some findings from this research that were relevant to the Northwest Climate Adaptation Science Center-funded work. Additionally, we are currently preparing two peer-reviewed manuscripts that were partially supported by this funding. We plan to coordinate with Cory Davis (NRFSN Science Communication Specialist) to schedule a NRFSN webinar communicating these results and have plans to develop a NRFSN research brief following publication of our manuscripts in 2023.

Conclusions, Implications for Management/Policy, and Future Research

Our results demonstrate that spatial patterns of burn severity scale consistently with fire size within contemporary Northwest US fire regimes. These spatial scaling relationships, which appear stationary across space and time, offer a means to infer future patterns of burn severity, particularly in climate-limited fire regimes where empirical data are inherently lacking. As fire size distributions shift to the right (i.e., increase in size), our findings illustrate that the size and spatial homogeneity of high-severity burned patches will also consistently increase, carrying implications for forest resilience in a period of increasing fire activity. In the western US, increasing aridity in recent decades has been linked to both increasing annual area burned as well as increasing fire event sizes (Juang *et al.* 2022), and these trends are expected to continue (Parks & Abatzoglou 2020). In forest ecosystems, the increasing size and homogeneity of high-severity patches will directly impact seed dispersal (Gill *et al.* 2022), rates of tree regeneration (Harvey *et al.* 2016b), and the potential for conversion to non-forest systems (Coop *et al.* 2020) following fire.

Within the Northwest US, spatial patterns of burn severity appear consistent across regions with distinct biophysical characteristics yet similarly climate-limited fire regimes (i.e., the Pacific Northwest and the Northern Rockies). While this finding implies that insights about expected burn severity patterns may be shared across regions, the implications of these patterns must be considered in the context of the unique biophysical characteristics of each region. Comparable burn severity patterns occurring in distinct regions can lead to varying forest regeneration trajectories, depending on the fire-adapted traits of dominant tree species (Harvey *et al.* 2016b; Littlefield 2019). Serotinous lodgepole pine (*Pinus contorta* var *latifolia*), which is prevalent in the Northern Rockies (Hood *et al.* 2021), can facilitate rapid and dense tree regeneration following fire, even in the interior portions of high-severity burn patches (Turner *et al.* 2003; Harvey *et al.* 2016b). Serotiny is found in scattered lodgepole pine populations in the Pacific Northwest, but is primarily restricted to the highest elevations, and dispersal of seeds from unburned live source is instead the primary mechanism of tree regeneration in this region following fire (Reilly *et al.* 2021). Therefore, a given burn-severity mosaic might be expected to lead to substantially slower forest recovery trajectories in the Pacific Northwest compared to the Northern Rockies, particularly within the interior portions of the largest high-severity burned patches. Planning for post-fire replanting in these areas will be important where maintaining forest cover is the management goal.

Our findings highlight the need for future research directions. First, although some of the largest increases in annual area burned are expected to occur in historically climate-limited fire regimes (Littell *et al.* 2018; McColl-Gausden *et al.* 2022), the magnitude of potential fire size distribution shifts are less understood. In the Western Cascades, for example, the largest fire events are typically driven by synoptic east wind events (Donato *et al.* 2020; Reilly *et al.* 2022), and it is still unclear whether and how the frequency of these events might shift moving forward. As refined projections for fire size distributions become available, such information can be linked with the approach presented here to provide plausible estimates of potential future burn severity impacts. Second, although we observed stationarity in scaling relationships within the contemporary record, future shifts in climate and fire activity may lead to increasing fuel limitations in areas subject to increasing fire (Kennedy *et al.* 2021; Turner *et al.* 2022). Such shifts may lead to shifts in the envelopes of potential burn severity patterns in the future. Continued implementation of the methods presented here would permit such changes to be detected (e.g., downward shifts in scaling relationships might suggest an increasing prevalence of local-scale fuel constraints, thereby signaling potentially important changes in fire regimes), signaling important future changes in the nature of fire regimes.

Literature Cited

Abatzoglou, J.T., Rupp, D.E., O'Neill, L.W. & Sadegh, M. (2021). Compound Extremes Drive the Western Oregon Wildfires of September 2020. *Geophysical Research Letters*, 48.

Agee, J.K. (1993). *Fire ecology of Pacific Northwest forests*. Island Press, Washington, DC.

Arienti, M.C., Cumming, S.G. & Boutin, S. (2006). Empirical models of forest fire initial attack success probabilities: the effects of fuels, anthropogenic linear features, fire weather, and management. *Can. J. For. Res.*, 36, 3155–3166.

Baker, W.L. (2009). *Fire ecology in Rocky Mountain landscapes*. Island Press, Washington, DC.

Cade, B.S. & Noon, B.R. (2003). A gentle introduction to quantile regression for ecologists. *Frontiers in Ecology and the Environment*, 1, 412–420.

Cansler, C.A. & McKenzie, D. (2014). Climate, fire size, and biophysical setting control fire severity and spatial pattern in the northern Cascade Range, USA. *Ecological Applications*, 24, 1037–1056.

Clarke, H., Penman, T., Boer, M., Cary, G.J., Fontaine, J.B., Price, O., *et al.* (2020). The Proximal Drivers of Large Fires: A Pyrogeographic Study. *Front. Earth Sci.*, 8, 90.

Collins, B.M., Stevens, J.T., Miller, J.D., Stephens, S.L., Brown, P.M. & North, M.P. (2017). Alternative characterization of forest fire regimes: incorporating spatial patterns. *Landscape Ecol*, 32, 1543–1552.

Commission for Environmental Cooperation. (1997). *Ecological regions of North America: toward a common perspective*.

Coop, J.D., Parks, S.A., Stevens-Rumann, C.S., Crausbay, S.D., Higuera, P.E., Hurteau, M.D., *et al.* (2020). Wildfire-Driven Forest Conversion in Western North American Landscapes. *BioScience*, 70, 659–673.

Donato, D.C., Fontaine, J.B., Campbell, J.L., Robinson, W.D., Kauffman, J.B. & Law, B.E. (2009). Conifer regeneration in stand-replacement portions of a large mixed-severity wildfire in the Klamath–Siskiyou Mountains. *Can. J. For. Res.*, 39, 823–838.

Donato, D.C., Halofsky, J.S. & Reilly, M.J. (2020). Corralling a black swan: natural range of variation in a forest landscape driven by rare, extreme events. *Ecol Appl*, 30.

Fromm, M., Lindsey, D.T., Servranckx, R., Yue, G., Trickl, T., Sica, R., *et al.* (2010). The Untold Story of Pyrocumulonimbus. *Bull. Amer. Meteor. Soc.*, 91, 1193–1210.

Gill, N.S., Turner, M.G., Brown, C.D., Glassman, S.I., Haire, S.L., Hansen, W.D., *et al.* (2022). Limitations to Propagule Dispersal Will Constrain Postfire Recovery of Plants and Fungi in Western Coniferous Forests. *BioScience*, 72, 347–364.

Hagmann, R.K., Hessburg, P.F., Prichard, S.J., Povak, N.A., Brown, P.M., Fulé, P.Z., *et al.* (2021). Evidence for widespread changes in the structure, composition, and fire regimes of western North American forests. *Ecological Applications*, 31.

Halofsky, J.E., Peterson, D.L. & Harvey, B.J. (2020). Changing wildfire, changing forests: the effects of climate change on fire regimes and vegetation in the Pacific Northwest, USA. *fire ecol*, 16, 4.

Halofsky, J.S., Donato, D.C., Franklin, J.F., Halofsky, J.E., Peterson, D.L. & Harvey, B.J. (2018). The nature of the beast: examining climate adaptation options in forests with stand-replacing fire regimes. *Ecosphere*, 9, e02140.

Hantson, S., Pueyo, S. & Chuvieco, E. (2016). Global fire size distribution: from power law to log-normal. *Int. J. Wildland Fire*, 25, 403.

Harvey, B.J., Donato, D.C. & Turner, M.G. (2016a). Drivers and trends in landscape patterns of stand-replacing fire in forests of the US Northern Rocky Mountains (1984–2010). *Landscape Ecol*, 31, 2367–2383.

Harvey, B.J., Donato, D.C. & Turner, M.G. (2016b). High and dry: post-fire tree seedling establishment in subalpine forests decreases with post-fire drought and large stand-replacing burn patches: Drought and post-fire tree seedlings. *Global Ecol. Biogeogr.*, 25, 655–669.

Hijmans, R.J., van Etten, J., Sumner, M., Cheng, J., Baston, D., Bevan, A., *et al.* (2022). Package "raster."

Hood, S.M., Harvey, B.J., Fornwalt, P.J., Naficy, C.E., Hansen, W.D., Davis, K.T., *et al.* (2021). Fire Ecology of Rocky Mountain Forests. In: *Fire Ecology and Management: Past, Present, and Future of US Forested Ecosystems*, Managing Forest Ecosystems (eds. Greenberg, C.H. & Collins, B.). Springer International Publishing, Cham, pp. 287–336.

Juang, C.S., Williams, A.P., Abatzoglou, J.T., Balch, J.K., Hurteau, M.D. & Moritz, M.A. (2022). Rapid Growth of Large Forest Fires Drives the Exponential Response of Annual Forest-Fire Area to Aridity in the Western United States. *Geophysical Research Letters*, 49.

Kennedy, M.C., Bart, R.R., Tague, C.L. & Choate, J.S. (2021). Does hot and dry equal more wildfire? Contrasting short- and long-term climate effects on fire in the Sierra Nevada, CA. *Ecosphere*, 12.

Koenker, R. & Bassett, G. (1978). Regression quantiles. *Econometrica*.

Littell, J.S., McKenzie, D., Peterson, D.L. & Westerling, A.L. (2009). Climate and wildfire area burned in western U.S. ecoprovinces, 1916–2003. *Ecological Applications*, 19, 1003–1021.

Littell, J.S., McKenzie, D., Wan, H.Y. & Cushman, S.A. (2018). Climate Change and Future Wildfire in the Western United States: An Ecological Approach to Nonstationarity. *Earth's Future*, 6, 1097–1111.

Littlefield, C.E. (2019). Topography and post-fire climatic conditions shape spatio-temporal patterns of conifer establishment and growth. *fire ecol*, 15, 34.

McColl-Gausden, S.C., Bennett, L.T., Clarke, H.G., Ababei, D.A. & Penman, T.D. (2022). The fuel–climate–fire conundrum: How will fire regimes change in temperate eucalypt forests under climate change? *Global Change Biology*, 28, 5211–5226.

McKenzie, D. & Kennedy, M.C. (2011). Scaling Laws and Complexity in Fire Regimes. In: *The Landscape Ecology of Fire*, Ecological Studies (eds. McKenzie, D., Miller, C. & Falk, D.A.). Springer Netherlands, Dordrecht, pp. 27–49.

McKenzie, D. & Kennedy, M.C. (2012). Power laws reveal phase transitions in landscape controls of fire regimes. *Nat Commun*, 3, 726.

Miller, J.D., Safford, H.D., Crimmins, M. & Thode, A.E. (2009). Quantitative Evidence for Increasing Forest Fire Severity in the Sierra Nevada and Southern Cascade Mountains, California and Nevada, USA. *Ecosystems*, 12, 16–32.

Miller, J.D. & Thode, A.E. (2007). Quantifying burn severity in a heterogeneous landscape with a relative version of the delta Normalized Burn Ratio (dNBR). *Remote Sensing of Environment*, 109, 66–80.

Moritz, M.A., Hessburg, P.F. & Povak, N.A. (2011). Native Fire Regimes and Landscape Resilience. In: *The Landscape Ecology of Fire*, Ecological Studies (eds. McKenzie, D., Miller, C. & Falk, D.A.). Springer Netherlands, Dordrecht, pp. 51–86.

Muggeo, V.M.R. (2021). Additive Quantile regression with automatic smoothness selection: the R package quantregGrowth.

Muggeo, V.M.R., Torretta, F., Eilers, P.H.C., Sciandra, M. & Attanasio, M. (2021). Multiple smoothing parameters selection in additive regression quantiles. *Statistical Modelling*, 21, 428–448.

Parks, S., Holsinger, L., Voss, M., Loehman, R. & Robinson, N. (2018a). Mean Composite Fire Severity Metrics Computed with Google Earth Engine Offer Improved Accuracy and Expanded Mapping Potential. *Remote Sensing*, 10, 879.

Parks, S.A. & Abatzoglou, J.T. (2020). Warmer and Drier Fire Seasons Contribute to Increases in Area Burned at High Severity in Western US Forests From 1985 to 2017. *Geophysical Research Letters*, 47.

Parks, S.A., Holsinger, L.M., Panunto, M.H., Jolly, W.M., Dobrowski, S.Z. & Dillon, G.K. (2018b). High-severity fire: evaluating its key drivers and mapping its probability across western US forests. *Environ. Res. Lett.*, 13, 044037.

Pausas, J.G., Keeley, J.E. & Schwilk, D.W. (2017). Flammability as an ecological and evolutionary driver. *J Ecol*, 105, 289–297.

Pebesma, E. (2018). Simple Features for R: Standardized Support for Spatial Vector Data. *The R Journal*, 10, 439.
Peters, D.P.C., Pielke, R.A., Bestelmeyer, B.T., Allen, C.D., Munson-McGee, S. & Havstad, K.M. (2004). Cross-scale interactions, nonlinearities, and forecasting catastrophic events. *Proc. Natl. Acad. Sci. U.S.A.*, 101, 15130–15135.
Povak, N.A., Hessburg, P.F. & Salter, R.B. (2018). Evidence for scale-dependent topographic controls on wildfire spread. *Ecosphere*, 9.
Prichard, S.J., Povak, N.A., Kennedy, M.C. & Peterson, D.W. (2020). Fuel treatment effectiveness in the context of landform, vegetation, and large, wind-driven wildfires. *Ecol Appl*, 30.
Pueyo, S. (2006). Diversity: between neutrality and structure. *Oikos*, 112, 392–405.
Pueyo, S. (2014). Algorithm for the maximum likelihood estimation of the parameters of the truncated normal and lognormal distributions.
Reilly, M.J., Dunn, C.J., Meigs, G.W., Spies, T.A., Kennedy, R.E., Bailey, J.D., *et al.* (2017). Contemporary patterns of fire extent and severity in forests of the Pacific Northwest, USA (1985-2010). *Ecosphere*, 8, e01695.
Reilly, M.J., Halofsky, J.E., Krawchuk, M.A., Donato, D.C., Hessburg, P.F., Johnston, J.D., *et al.* (2021). Fire Ecology and Management in Pacific Northwest Forests. In: *Fire Ecology and Management: Past, Present, and Future of US Forested Ecosystems*, Managing Forest Ecosystems (eds. Greenberg, C.H. & Collins, B.). Springer International Publishing, Cham, pp. 393–435.
Reilly, M.J., Zuspan, A., Halofsky, J.S., Raymond, C., McEvoy, A., Dye, A.W., *et al.* (2022). Cascadia Burning: The historic, but not historically unprecedented, 2020 wildfires in the Pacific Northwest, USA. *Ecosphere*, 13.
Rollins, M.G. (2009). LANDFIRE: a nationally consistent vegetation, wildland fire, and fuel assessment. *Int. J. Wildland Fire*, 18, 235.
Rose, N.L., Yang, H., Turner, S.D. & Simpson, G.L. (2012). An assessment of the mechanisms for the transfer of lead and mercury from atmospherically contaminated organic soils to lake sediments with particular reference to Scotland, UK. *Geochimica et Cosmochimica Acta*, 82, 113–135.
Saberi, S.J. (2019). Quantifying burn severity in forests of the interior Pacific Northwest: From field measurements to satellite spectral indices. Master's Thesis. University of Washington.
Scaduto, E., Chen, B. & Jin, Y. (2020). Satellite-Based Fire Progression Mapping: A Comprehensive Assessment for Large Fires in Northern California. *IEEE J. Sel. Top. Appl. Earth Observations Remote Sensing*, 13, 5102–5114.
Stevens, J.T., Collins, B.M., Miller, J.D., North, M.P. & Stephens, S.L. (2017). Changing spatial patterns of stand-replacing fire in California conifer forests. *Forest Ecology and Management*, 406, 28–36.
Stevens, J.T., Kling, M.M., Schwilk, D.W., Varner, J.M. & Kane, J.M. (2020). Biogeography of fire regimes in western U.S. conifer forests: A trait-based approach. *Global Ecol Biogeogr*, 29, 944–955.
Turner, M.G., Braziunas, K.H., Hansen, W.D., Hoecker, T.J., Rammer, W., Ratajczak, Z., *et al.* (2022). The magnitude, direction, and tempo of forest change in Greater Yellowstone in a warmer world with more fire. *Ecological Monographs*, 92.

Turner, M.G., Romme, W.H. & Tinker, D.B. (2003). Surprises and lessons from the 1988 Yellowstone fires. *Frontiers in Ecology and the Environment*, 1, 351–358.
Westerling, A.L. (2016). Increasing western US forest wildfire activity: sensitivity to changes in the timing of spring. *Phil. Trans. R. Soc. B*, 371, 20150178.
Westerling, A.L., Hidalgo, H.G., Cayan, D.R. & Swetnam, T.W. (2006). Warming and Earlier Spring Increase Western U.S. Forest Wildfire Activity. *Science*, 313, 940–943.

Appendix A: Contact Information for Key Project Personnel

Michele S. Buonanduci, Student Investigator:

School of Environmental and Forest Sciences
University of Washington
Box 352100
Seattle, WA 98195-2100
School of Environmental and Forest Sciences
University of Washington

Email: mbuon@uw.edu
Phone: (206) 616-1879

Dr. Brian J. Harvey, Principal Investigator:

School of Environmental and Forest Sciences
University of Washington
Box 352100
Seattle, WA 98195-2100
School of Environmental and Forest Sciences
University of Washington

Email: bjharvey@uw.edu
Phone: (206) 685-9929

Appendix B: List of Completed/Planned Scientific/Technical Publications/Science Delivery Products

Deliverable type	Description	Delivery date
Webinar and conference presentations	**Buonanduci, M.S.**, D.C. Donato, J.S. Halofsky, M.C. Kennedy, and B.J. Harvey. 2023. Fire Science Exchange Network webinar with the Northern Rockies Fire Science Network (NRFSN).	Planned for fall/winter 2023
	Buonanduci, M.S., D.C. Donato, J.S. Halofsky, M.C. Kennedy, and B.J. Harvey. 2023. Examining wildfires from other regions and fire regimes yields insights into future patterns of burn severity in western Cascadia. Oregon Post-Fire Research and Monitoring Symposium. Oral presentation.	February 2023
	Buonanduci, M.S., D.C. Donato, J.S. Halofsky, M.C. Kennedy, and B.J. Harvey. 2022. Western Cascadia wildfire: spatial patterns of burn severity and implications for future ecological impacts. University of Washington School of Aquatic and Fishery Sciences Quantitative Seminar Series. Invited oral presentation.	May 2022
	Buonanduci, M.S., D.C. Donato, J.S. Halofsky, and B.J. Harvey. 2021. Potential impacts of future fires in western Cascadia: scaling spatial patterns of burn severity. International Fire Ecology and Management Congress. Oral presentation.	November 2021
Report	**Buonanduci, M.S.** and B.J. Harvey. 2022. Potential impacts of future fires in the western Cascades: insights from spatial metrics of burn severity. Final report to the Northwest Climate Adaptation Science Center.	August 2022
Refereed publications	**Buonanduci, M.S.**, D.C. Donato, J.S. Halofsky, M.C. Kennedy, and B.J. Harvey. In prep. Consistent spatial scaling of high-severity wildfire can inform expected future patterns of burn severity.	In review; submitted February 2023
	Buonanduci, M.S., D.C. Donato, J.S. Halofsky, M.C. Kennedy, and B.J. Harvey. In prep. Scaling of severe fire patterns across forest ecosystems yields insights for a data-sparse and infrequent-fire regime.	Submission planned May 2023
Doctoral dissertation	M.S. Buonanduci will defend her dissertation and graduate in June 2023.	Planned for June 2023

Appendix C: Metadata

The data generated for this project reflect the spatial characteristics of burn severity patterns within 1,615 fire events occurring across the Northwest US between 1985 and 2020. The burn severity dataset includes details such as fire year, fire regime group, geographic region, and high-severity patch metrics for each fire event ("NW_fire_spatial_metrics.csv").

The dataset is accompanied by metadata following standards specified in the Ecological Metadata Language (EML, http://lternet.edu/wp-content/uploads/2010/12/EMLHandbook-2.pdf), which is used widely. This format is appropriate for statistical analyses using tools in R. Spatial data sets are documented using the FGDC Content Standard for Digital Geospatial Metadata. The data and associated metadata are planned for archival in the Forest Service Research Data Archive upon the publication of a peer-reviewed journal article presenting the data.